

CNWRA A center of excellence in earth sciences and engineering

A Division of Southwest Research Institute™
6220 Culebra Road • San Antonio, Texas, U.S.A. 78228-5166
(210) 522-5160 • Fax (210) 522-5155

October 31, 2001
Contract No. NRC-02-97-009
Account No. 20.01402.571

U.S. Nuclear Regulatory Commission
ATTN: Mrs. Deborah A. DeMarco
Two White Flint North
11545 Rockville Pike
Mail Stop T8 A23
Washington, DC 20555

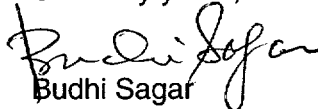
Subject: Programmatic review of the paper titled "Effect of Oxide Thickness on the Localized Corrosion of Zircaloy" for presentation at the NACE CORROSION 2002 Conference

Dear Mrs. DeMarco:

Attached is the subject paper to be presented at the NACE CORROSION 2002 Conference to be held on April 7–12, 2002 in Denver, CO. The paper is focused on the localized corrosion of Zircaloy, the alloy used as fuel rod cladding in commercial nuclear power reactor, and discussed the role of environmental factors and hydrothermally grown oxide layers on the initiation of pitting corrosion under disposal conditions. A portion of the information presented in this paper has been abstracted from IM 01402.571.180 titled "Effect of In-Package Chemistry on the Degradation of Vitrified High-Level Radioactive Waste and Spent Nuclear Fuel Cladding" (CNWRA 2002-01) and has been previously approved by the NRC staff.

Please contact Sean Brossia at (210) 522-5797 or Gustavo Cragnoilino (210) 522-5539 if you have any questions regarding this paper.

Sincerely yours,


Budhi Sagar
Technical Director

BS:SB:jg

Enclosure

cc:	J. Linehan	K. Stablein	D. Brooks	T. Essig	G. Cragnoilino
	B. Meehan	B. Leslie	T. McCartin	A. Henry	S. Brossia
	E. Whitt	T. Ahn	T. Bloomer	W. Patrick	D. Dunn
	J. Greeves	C. Greene	J. Andersen	CNWRA Dirs.	P. Maldonado
	J. Piccone	S. Wastler	J. Thomas	CNWRA EMs	T. Nagy (contracts)



Washington Office • Twinbrook Metro Plaza #210
12300 Twinbrook Parkway • Rockville, Maryland 20852-1606

Effect of Oxide Thickness on the Localized Corrosion of Zircaloy

C.S. Brossia, G.A. Cragnolino, D.S. Dunn
Center for Nuclear Waste Regulatory Analyses
Southwest Research Institute
San Antonio, TX

ABSTRACT

Zircaloy (-2 and -4) spent nuclear fuel cladding is considered by the U. S. Department of Energy as an additional metallic barrier for the containment of radionuclides in the proposed repository at Yucca Mountain, Nevada. Because Zircaloy develops a thick oxide during in-reactor service, hydrothermally oxidized Zircaloy was compared to as-polished Zircaloy under a variety of environmental conditions to evaluate the effect of the oxide film on localized (pitting) corrosion in chloride-containing solutions. Besides cyclic potentiodynamic polarization and potentiostatic tests, open circuit potentials measurements were conducted in air saturated chloride solutions with the addition of H_2O_2 and $FeCl_3$. The electrical characteristics of the hydrothermally grown oxide films were examined using electrochemical impedance spectroscopy and measurements of the charge transfer resistance for a redox couple. Stable pitting corrosion in the presence of a thick oxide layer was observed after 40 days in potentiostatic tests but it was not initiated in open circuit tests. Preliminary explanations for this observation are provided.

INTRODUCTION

A large portion of the commercial spent nuclear fuel to be disposed in the proposed repository at Yucca Mountain, Nevada, is clad with Zircaloy-2 (Zr-2)⁽¹⁾ or Zircaloy-4 (Zr-4)⁽²⁾. These two Zr-1.5%Sn alloys contain Fe, Cr, and Ni as minor alloying elements but differ in that the Ni content is much lower in Zr-4 to decrease the hydrogen pick-up as a result of corrosion in high temperature water. For this reason, Zr-4 is used in pressurized water reactors (PWRs) whereas Zr-2 is used for boiling water reactor (BWR) fuel cladding. The U.S. Department of Energy (DOE), in its performance assessment of the proposed repository, has assumed that Zr-2 or Zr-4 cladding an additional metallic barrier to radionuclide release.¹

Zr alloys, and in particular Zr-2 and Zr-4, exhibit exceptional corrosion resistance in a variety of aqueous solutions over a wide range of pHs and temperatures due to the formation of a protective passive film composed of ZrO_2 . However, Zr and its alloys are known to be susceptible to various degradation modes as a result of aqueous corrosion that may lead to the failure of fuel cladding under disposal conditions, including general corrosion, localized corrosion, and stress corrosion cracking. Of the species expected to be present in the

⁽¹⁾UNS R60802.

⁽²⁾UNS R60804.

groundwater at Yucca Mountain, chloride and fluoride anions are considered to likely to have the most significant effect on localized corrosion of Zr-2 or Zr-4.

In previous work,² we have examined the general and localized corrosion of as-polished Zr-4 in an attempt to try to understand the possible failure modes that may be encountered in the proposed repository at Yucca Mountain. It was observed that pitting corrosion occurs in both neutral and acidic chloride solutions above a critical potential. As reviewed elsewhere,³ the critical potential for pitting initiation measured using potentiostatic techniques combined with mechanical disruption of the passive film by straining and scratching coincides with the repassivation potential (E_{rp}). E_{rp} also exhibits a linear dependence with the logarithm of the chloride concentration.

Zircaloy cladding, however, undergoes significant oxidation while in service and the behavior of as-polished material may not be representative of actual cladding. For example, the oxide film on spent nuclear fuel cladding typically has a thickness ranging from 10 to 60 μm as a result of oxidation during the fuel cycle under reactor operating conditions.⁴ Thus, the purpose of this work was to examine the localized corrosion of hydrothermally oxidized Zr-4 under conditions similar to those used previously to study as-polished Zr-4.

EXPERIMENTAL PROCEDURES

All tests were performed using a single heat of Zr-4, whose chemical composition is shown in Table 1. Specimens were machined from an annealed 9.5 mm thick plate in the form of cylinders 6.3 mm in diameter and 48.6 mm in length. The specimens were wet polished to a 600 grit finish prior to oxidizing. Hydrothermal oxidation was conducted in deionized (DI) water inside an autoclave at 300 °C for periods of 2, 4, 8, and 12 weeks. Based on the weight gain, and using the relationship provided by Hillner et al.,⁵ approximate oxide thicknesses for the various exposure periods were calculated and listed in Table 2.

Table 1. Composition of Zr-4 Utilized in Current Study (in wt %)

Sn	Fe	Cr	Ni	O (ppm)	Zr
1.51	0.20	0.10	0.0035	1420	bal.

Table 2. Weight Gain and Resulting Oxide Thickness During Hydrothermal Oxidation of Zr-4. Thickness Calculated from Weight Change Using Relationship Provided by Hillner et al.⁵

Exposure Time (weeks)	Weight Gain (mg)	Weight Gain/Unit Area (mg/dm^2)	Thickness (μm)
2	2.06	25.12	1.7
4	3.28	40.01	2.7
8	3.87	47.19	3.2
12	4.16	50.68	3.4

Initial tests were performed in chloride solutions containing 0.25 mM sulfate (SO_4^{2-}), 0.16 mM nitrate (NO_3^-), 0.10 mM fluoride (F^-) and a total carbonate ($\text{HCO}_3^- + \text{CO}_3^{2-}$) concentration of 1.4 mM, in order to simulate the chemical composition of the groundwater in the vicinity of Yucca Mountain as represented by J-13 well water. The presence of these additional anions, however, was shown to have only a minimal effect on the corrosion behavior of Zr-4 in the presence of chloride concentrations above 1 mM and thus was excluded from further use.² The chloride concentrations examined ranged from 1mM to 4M. All solutions were prepared using reagent grade sodium salts and 18 $\text{M}\Omega\cdot\text{cm}$ water. The tests were conducted at 25, 65, and 95 °C. The solution was purged with high purity N_2 and heated to the desired temperature. The specimen was then introduced into the cell and the test was initiated after measuring the initial rest potential.

Both cyclic potentiodynamic polarization (CPP) and potentiostatic tests were performed to examine the conditions under which localized corrosion of Zr-4 takes place. All tests were conducted using a saturated calomel reference electrode (SCE) maintained at room temperature and connected to the cell through a salt bridge/Luggin probe filled with either 100 mM or 1 M chloride solution depending on the concentration of the testing solution. A platinum foil was used as a counter electrode. CPP tests were initiated at 0.1 V less than the open circuit potential after the specimen had been immersed in solution for an adequate period of time such that a steady state corrosion potential, E_{corr} , was reached. A potential scan rate of 0.167 mV/s was used and the scans were reversed when a current density of 5 mA/cm² was reached.

A series of open circuit potential measurements were also conducted to examine the possibility of exceeding the critical potentials for localized corrosion under naturally corroding conditions. These tests were performed in air-saturated solutions, in which synthetic (CO₂-free) air was purged continuously into the cell. The tests also involved, after a steady potential was reached, the addition of hydrogen peroxide and ferric chloride to enhance the oxidizing power of the solution.

Additional experiments were also used in an effort to characterize the oxide in an attempt to try to explain differences observed between the as-polished and oxidized specimens. Electrochemical impedance spectroscopy (EIS) was conducted in the passive regime of Zr-4 by applying a potential of -0.25 V_{SCE} and superimposing a 10 mV amplitude sinusoidal potential wave in deaerated, 0.1 M NaCl at 95 °C. In addition, the relative electronic conductivity of these oxides was determined by comparing the linear polarization resistance measured for different oxide thicknesses in a deaerated 0.1 M Na₂SO₄ solution containing 0.1 M each of FeK₃(CN)₆ and FeK₄(CN)₆ in line with the approach suggested by Cerquetti et al.⁶ A potential variation of ± 20 mV with respect to the open circuit potential was used in these measurements.

RESULTS

As shown in Figure 1, the plot of E_{rp} as a function of chloride concentration for the polished specimens in tests conducted in the simulated J-13 water (pH 8.4) exhibits a linear logarithmic dependence on chloride concentration, given by

$$E_{\text{rp}} = E_{\text{rp}}^0 - B \log[\text{Cl}^-] \quad (\text{Eq. 1})$$

where E_{rp}^0 is the repassivation potential at a chloride concentration of 1 M and B is the slope of the dependence of the repassivation potential on the logarithm of the chloride concentration. Both B and E_{rp}^0 were observed to be temperature independent over the range of 25 – 95 °C and had values of 0.083 mV/decade-[Cl⁻] and 0.04 V_{SCE}.² Importantly, however, E_{rp} in 0.1 M chloride solutions at 95 °C for hydrothermally oxidized specimens with thicknesses of 1.7 and 3.4 μm is almost (close to the lower bound of the 99% confidence interval) equal to that for the as polished specimens at the same chloride concentration and temperature.

The effect of the hydrothermally grown oxide film thickness on the initiation time for pitting corrosion under potentiostatic conditions is shown in Figure 2. This figure shows plots of the anodic current density as a function of time in 0.1 M NaCl solution at 95 °C and an applied potential of 0.125 V_{SCE} for specimens covered with oxide films ranging from 1.7 to 3.4 μm as compared to the plot for a polished specimen. It is clearly illustrated in Figure 2 that, at a potential that is only 15 to 25 mV above E_{rp} , the initiation time for pitting corrosion, as indicated by the abrupt jump in current density from a very low value, increased significantly with oxide film thickness. Pit initiation eventually occurred, but more than 40 days were required to induce pitting corrosion in the specimen with the thickest oxide compared to few minutes for the polished specimen. Even though it is not evident as a result of the scale used in Figure 2, the current density measured before passivity breakdown was about 10⁻⁸ A/cm² and almost independent of oxide film thickness, with the single exception of the specimen with an oxide film thickness of 3.2 μm, which exhibited pronounced current fluctuations from the beginning of the potentiostatic test.

Plots of the evolution of E_{corr} of Zr-4 in air-saturated 0.1 M NaCl at 95 °C, before and after the addition of H₂O₂ or FeCl₃ (attaining a concentration of 5 mM), are shown in Figure 3. Specimens covered with an oxide film hydrothermally grown to 1.7 and 3.4 μm were used in these tests. There are no clear trends in the evolution of E_{corr} during the initial 150 hours of exposure. Specimens with an oxide thickness of 1.7 μm exhibited an initial decay in E_{corr} followed by an increase, with a constant difference of approximately 300 mV between the values of E_{corr} for the two specimens. For the specimens with the thicker oxide film, the difference between the values of

E_{corr} was larger, approximately 450 mV, but the potential increased initially, reached a peak, and increased again after a minor decay. As expected, the E_{corr} values were found to be higher in average for the specimens with the thicker oxide film. After the addition of H_2O_2 , however, the values of E_{corr} became similar (< 100 mV difference) regardless of the oxide film thickness, reaching at the end of the test values close to those measured initially in the air saturated solution without H_2O_2 . On the other hand, E_{corr} values increased with the addition of FeCl_3 became higher, and remained relatively constant for the duration of the test. However, no pitting corrosion initiation was observed after approximately 840 hours (~ 35 days) on the specimens exposed under open circuit potential conditions to the chloride solution after the addition of FeCl_3 even though the E_{corr} values (differing in ~300 mV for these two specimens with different oxide thickness) were higher than E_{rp} . No potential decay associated with the activation of the specimen as a result of corrosion was noted in agreement with the microscopic examination. In the chloride solution containing H_2O_2 the E_{corr} values were close to E_{rp} , and pitting corrosion was not initiated, suggesting that a certain over potential is needed to promote pitting under open circuit conditions.

To better understand the nature of the oxide films, their electronic properties were examined by measuring the exchange current density associated with the $\text{Fe}(\text{CN})_6^{3-}/\text{Fe}(\text{CN})_6^{4-}$ redox couple. By conducting a linear polarization measurement, the charge transfer resistance of the redox reactions can be ascertained, using the expression shown in Eq. 2

$$i_o = \frac{RT}{zF} \frac{1}{R_t} \quad (\text{Eq. 2})$$

where i_o is the exchange current density, R is the universal gas constant, T is temperature, z is the charge transfer, F is Faraday's constant and R_t is the measured charge transfer resistance. The measured polarization resistance, equivalent in this case to the charge transfer resistance, is shown in Figure 4 as a function of oxide thickness. In this case, the as-polished air-formed film is assigned a thickness value of 0 μm . For the as-polished condition, a polarization resistance of just over $10^4 \Omega$ is observed. Increasing the oxide thickness to 1.7 and 3.4 μm resulted in increasing the polarization resistance to 2.4×10^5 and $3.2 \times 10^7 \Omega$. Using Eq. 2, these values translate to exchange current densities of 2.9×10^{-7} , 1.4×10^{-8} , and $1.0 \times 10^{-10} \text{ A/cm}^2$, respectively.

EIS was also used to characterize the oxide films and the results are shown in Figures 5 – 7. Also shown in the figures are the fitting results when the circuit model shown in Figure 8 was utilized. The EIS results showed increases in the resistive component of the Warburg impedance with increases in oxide thickness. For example, the as-polished and 3.4 μm oxide specimens had Warburg resistances of 1.9×10^6 and 1.4×10^7 . Furthermore, the calculated film capacitance decreased with increasing oxide thickness, as expected for a single plate capacitor, going from 150 μF for the air-formed oxide down to 0.3 μF for the 3.4 μm thick oxide.

Additional experiments were also conducted examining the effects of galvanically coupling bare, as-polished Zr-4 to oxidized Zr-4. The results of one such experiment are shown in Figure 9. Initially the current was cathodic with respect to the oxidized specimen at a value slightly greater than 10^{-5} A . The current subsequently decreased to very low values approaching 10^{-10} A before changing polarity and becoming anodic that then increased to a nominal value near 10^{-6} A after 400,000 seconds. The potential during this time period was fairly constant in the range of -0.30 to $-0.35 V_{\text{SCE}}$. After 445,860 seconds (~124 hr) FeCl_3 was added (point "A" in Figure 9) such that the total concentration was 0.5 mM. On the addition of the FeCl_3 , the potential abruptly increased to just over 0 V_{SCE} then decayed to approximately $-0.15 V_{\text{SCE}}$. Coincident with the potential jump, the current also jumped from $\sim 10^{-6}$ to $\sim 2 \times 10^{-5} \text{ A}$ before decaying back to 10^{-5} A . Further additions of FeCl_3 to increase the overall concentration to 1, 5, and 10 mM (labeled as "B", "C", and "D" in Figure 9) tended to result in some potential transients but these tended to decay and return to a nominally steady state potential around $-0.15 V_{\text{SCE}}$. The current similarly tended to exhibit transients followed by decaying values. The overall steady state current, however, was observed to increase with increasing concentrations of FeCl_3 reaching values on the order of $3 \times 10^{-5} \text{ A}$. Examination of the oxidized and as-polished specimens after exposure revealed that the as-polished specimen was essentially unchanged. The oxidized specimen, however, appeared to have developed several small, shallow pits at various locations.

DISCUSSION

As shown in Figure 1, E_{rp} for Zr-4 exhibits a linear dependence on the logarithm of the chloride concentration that extends from concentrations of the order of mM to values close to NaCl saturation. As noted,² the slope of this dependence, represented by B in Eq. 1, is approximately equal to 0.083 V/decade, a value similar to that reported by Maguire⁷ for commercially pure Zr and slightly higher than the theoretical value derived by Galvele in his model of pitting corrosion.⁸ The data shown in Figure 1 indicate that both B and E_{rp}° are independent of temperature practically up to the boiling point of water. This observation confirms that Zr-4, contrary to the case of many metals and alloys,^{9,10} does not exhibit a decrease in E_{rp} and E_{rp}° with increasing temperature in the range of 25 to 95 °C. As also shown in Figure 1, the presence of an oxide film with thickness estimated to range from 1.7 to 3.2 μm (see Table 2) does not affect the value of E_{rp} .

Though the presence of a thicker oxide film on Zr-4 does not seem to influence pit arrest, it is apparent that a thicker oxide significantly influences pit initiation process. This interpretation is confirmed by the results plotted in Figure 2. As indicated by the abrupt current rise, the pit initiation time at potentials just above E_{rp} increased significantly with increasing oxide layer thickness. It took about 42 days to initiate pitting corrosion when the oxide layer was about 3.4 μm thick. These results suggest that in the presence of thicker oxide films, such as those formed on spent nuclear fuel cladding, extremely long testing times may be required to initiate localized corrosion of Zircaloy. If sufficient time is allowed for pit initiation to occur, the difference between the breakdown potential (E_b) and E_{rp} tends to become negligible and justifies the use of E_{rp} as a useful threshold parameter that can be determined in a short-term electrochemical for predicting the occurrence of localized corrosion.^{2,11} On the contrary, E_b , determined from CPP testing, as many times has been reported,⁹ is not as useful a parameter because it is dominated by the random nature of the pit initiation process and therefore extremely dependent on experimental factors, such as surface preparation and roughness, potential scan rate, passivation times, and other test conditions. Some of these factors lead to E_b values significantly higher than E_{rp} . It should also be noted, in relation to the role of the thick hydrothermally grown oxide layer that the morphology of the localized attack changed substantially, as reported previously.¹¹

As noted in Figure 3, the addition of FeCl_3 increases E_{corr} above E_{rp} and can lead to the initiation of localized corrosion. However, it appears also from the results presented in Figure 3, that pitting corrosion is not easily initiated under open circuit conditions at least within the duration of these tests (42 days). One possibility is that the current supplied by the cathodic reduction of Fe^{3+} to Fe^{2+} ions (plus that resulting from the O_2 reduction) is not sufficient to promote pit initiation and growth because the ZrO_2 is a poor electronic conductor. To evaluate this further, the oxidation/reduction kinetics associated with the $\text{Fe}(\text{CN})_6^{3-}/\text{Fe}(\text{CN})_6^{4-}$ couple were studied on specimens of differing oxide thickness. As was shown in Figure 4, the resistance of the oxide to support external oxidation and reduction reactions increased significantly (over 3 orders of magnitude for the 3.4 μm case) when compared to the as-polished specimen with i_o for the $\text{Fe}(\text{CN})_6^{3-}/\text{Fe}(\text{CN})_6^{4-}$ redox couple decreasing from 2.9×10^{-7} to 1.0×10^{-10} A/cm^2 . These values for i_o are much less than those reported by Vetter¹² on Pt of 9×10^{-3} A/cm^2 and can be inferred from the work of Cerquetti et al.⁵ on Ti with values on the order of 10^{-5} A/cm^2 . EIS measurements (Figures 5-7) similarly revealed an increase in the oxide resistance with the resistive component of the Warburg impedance increasing by over an order of magnitude by comparing the as-polished to the 3.4 μm -thick oxide covered specimens. Furthermore, as the capacitance of the oxide film clearly increased with oxidation, this also supports the thought that the oxides were considerably thicker as well. These results clearly demonstrate the highly resistive nature of the oxides on Zr-4 to electronic conduction.

The concept of a cathodic limitation for pitting on the oxidized specimens was essentially confirmed when extremely shallow pitting ($< 3 \mu\text{m}$) was observed on an oxidized specimen coupled to an as-polished specimen only. Initially, the oxidized specimen was the cathode in this couple but after 48,000 seconds (~ 13 hrs) became the anode as shown in Figure 9. Prior to the addition of FeCl_3 , the couple potential and the net anodic current were relatively low and consistent with passive dissolution. After the addition of FeCl_3 , potential and current transients were observed. Some of these transients were clearly associated with the addition of the FeCl_3 to the environment. Other cases seem to indicate the onset of metastable pitting as evidenced by potential spikes. For Zr, if metastable pitting were occurring a change in the potential to that of E_{rp} would be expected. Thus, from a steady state potential on the order of $-0.05 V_{SCE}$ as observed after the total FeCl_3 reached 5 mM potential spikes to higher potentials would be expected and were observed. The peak potentials reached, however, were still below E_{rp} by approximately 30 to 60 mV. This could be an experimental artifact stemming from the data acquisition rate such that the peak potential did in fact reach E_{rp} but was not recorded. In any event, it is clear that by providing an alternative location for the cathodic reaction to take place that pitting of the oxidized Zr-4 can occur. Given this observation, however, it should be stressed that the pits were never sustained for any long

period of time (most transients were only a few minutes in duration) and the pits that were observed after testing were quite shallow. The observation of oxidized Zr failure when galvanically coupled to a material with a higher electronic conductivity that facilitates the cathodic reaction was reported by Cox.¹³ Cox observed SCC failures of an oxidized low-Ni variant of Zr-2 (similar to Zr-4) when galvanically coupled to Pt in 5% NaCl. Furthermore, Cox found that the potential at which failure occurred coincides with values comparable to E_{rp} because pitting corrosion is a precursor to SCC in the Zr/chloride system. It should also be noted, that the time to failure was over 16 weeks with some failures taking as long as a year. Thus, compared to the duration of the tests reported here, considerably longer tests may be needed to fully evaluate the possibility of localized corrosion of Zr-4.

To more completely evaluate the possibility of localized corrosion under anticipated repository conditions, there are a number of areas of further work that should be addressed. These include a further examination of other galvanic couples that may be encountered. One of these may be coupling of Zr-4 to stainless steel or carbon steel internal waste package components. Another area that should be addressed is an examination of the effects of fluoride on localized corrosion in combination with chloride. Additional work in the areas of better defining the possible chemical environment that may be present in terms of oxidizing species, possible inhibiting species, and the complexation reactions that may occur and might mitigate localized corrosion deserve attention.

CONCLUSIONS

- As-polished and oxidized Zr-4 are susceptible to pitting corrosion in chloride-containing solutions at concentrations above 0.001M and potentials higher than a repassivation potential which depends linearly on the logarithm of the chloride concentration but is temperature independent.
- Although the presence of a hydrothermally grown oxide film does not affect the value of the repassivation potential, it promotes a significant increase in the corrosion potential in air-saturated FeCl₃-containing solutions and increases the initiation time for pitting corrosion when potentiostatically polarized to potentials just above the repassivation potential.
- The corrosion potential of oxidized Zr-4 can reach the repassivation potential in FeCl₃-containing solutions and therefore pitting corrosion of fuel cladding may occur under natural corroding conditions inside a breached container. Studies on the kinetics of the cathodic reactions on oxide covered surfaces, however, seems to indicate that the conductivity of the oxide film is too low to support the current necessary to initiate and sustain propagation of localized corrosion.
- Additional studies are required to evaluate other conditions that may promote localized corrosion, including the effect of fluoride or mechanical action that may locally disrupt the integrity of the oxide film. Further efforts examining the possible inhibitory effects of the other anions present in the local groundwater is also warranted.

ACKNOWLEDGEMENTS

This paper was prepared to document work performed by the Center for Nuclear Waste Regulatory Analyses (CNWRA) for the U.S. Nuclear Regulatory Commission. Under Contract No. NRC-02-97-009. The activities reported here were performed on behalf of the NRC office of Nuclear Material Safety and Safeguards, Division of Waste Management. This paper is an independent product of CNWRA and does not necessarily reflect the views or the regulatory position of the NRC.

REFERENCES

1. U.S. Department of Energy, *Yucca Mountain Science and Engineering Report*, DOE/RWB0539, 2001.
2. C.A. Greene, C.S. Brossia, D.S. Dunn, and G.A. Cragolino, Environmental and Electrochemical Factors on the Localized Corrosion of Zircaloy-4, CORROSION/2000, paper no. 210 (Houston, TX: NACE International, 2000).

3. G.A. Cragolino, D.S. Dunn, C.S. Brossia, V. Jain, and K.S. Chan, Assessment of Performance Issues Related to Alternate Engineered Barrier System Materials and Design Options, CNWRA 99-003, 1999.
4. B. Cox, Degradation of Zirconium Alloys in Water Cooled Reactors, Third International Symposium on Environmental Degradation of Materials in Nuclear Power Systems - Water Reactors (Warrendale, PA: The Metallurgical Society, 1988), pp. 65-76.
5. E. Hillner, D.G. Franklin, and J.D. Smee, The Corrosion of Zircaloy-Clad Fuel Assemblies In a Geologic Repository Environment, WAPDBTB3173, 1994.
6. A. Cerquetti, F. Mazza, and M. Vigano, in Localized Corrosion, NACE-3, R.W. Staehle, B.F. Brown, J. Kruger, A. Agarwal, eds (Houston, TX: NACE International, 1974): p. 661
7. M. Maguire, The Pitting Susceptibility of Zirconium in Aqueous Cl⁻, Br⁻, and I⁻ Solutions, Industrial Applications of Titanium and Zirconium: Third Conference, ASTM STP 830 (Philadelphia, PA: American Society for Testing and Materials, 1984): pp. 175-189.
8. J.R. Galvele, Journal of the Electrochemical Society 123 (1976): pp. 464-474.
9. Z. Szklarska-Smialowska, Pitting Corrosion of Metals (Houston, TX: National Association of Corrosion Engineers, 1986).
10. G.A. Cragolino, A Review of Pitting Corrosion in High-Temperature Aqueous Solutions, Advances in Localized Corrosion (Houston, TX: National Association of Corrosion Engineers, 1990): pp. 413-431.
11. G. Cragolino, C.S. Brossia, D.S. Dunn and C.A. Greene. General and Localized Corrosion of Zircaloy Under High-Level Radioactive Waste Disposal Conditions. 10th International Conference on Environmental Degradation of Materials in Nuclear Power Systems -Water Reactors. Paper No. 105. Lake Tahoe, NV. August 5-9, 2001 (to be published by NACE International)
12. K.J. Vetter. Electrochemical Kinetics. Theoretical and Experimental Aspects (New York, NY: Academic Press, 1967).
13. B. Cox, Corrosion 29 (1973): pp. 157-166.

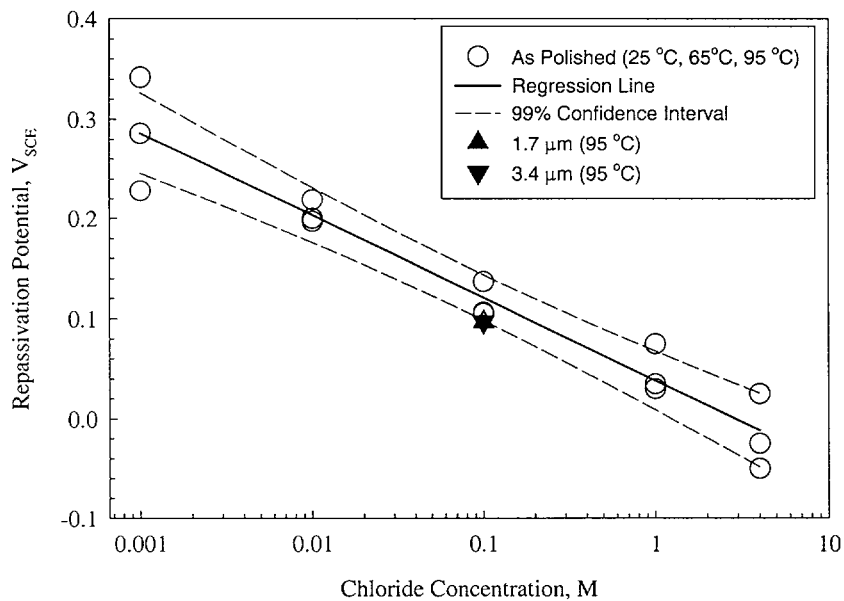


Figure 1: Effect of chloride concentration on the repassivation potential of as-polished and oxidized Zr-4.

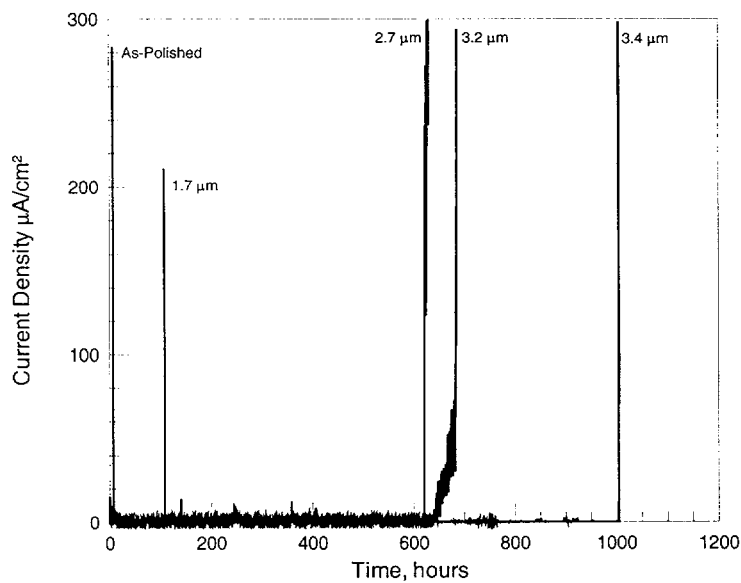


Figure 2: Potentiostatic polarization results for Zr-4 with varied oxide thicknesses in deaerated 0.1M NaCl solution at 95 °C and an applied potential of 0.125 V_{SCE} .

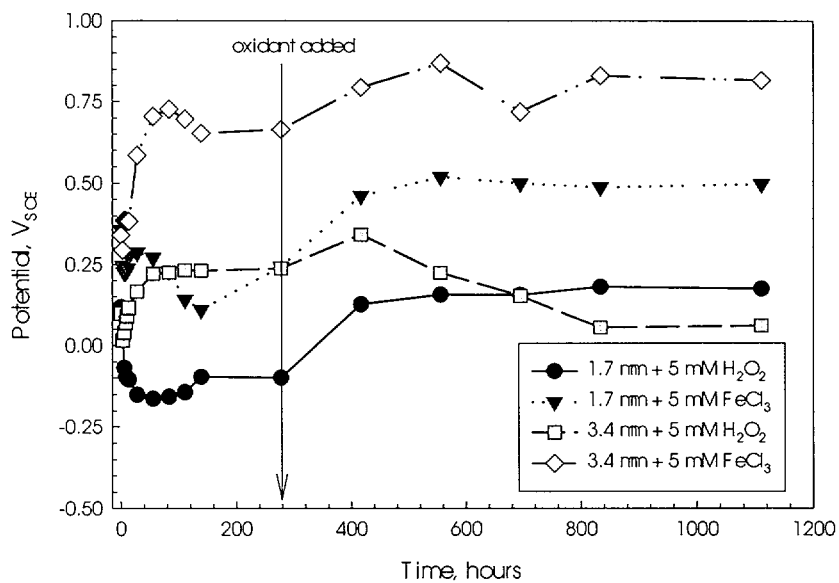


Figure 3: Open circuit measurements for oxidized Zr-4 in air-saturated 0.1M NaCl at 95 °C. Also shown are the effects of the addition of hydrogen peroxide and ferric chloride as additional oxidizing species.

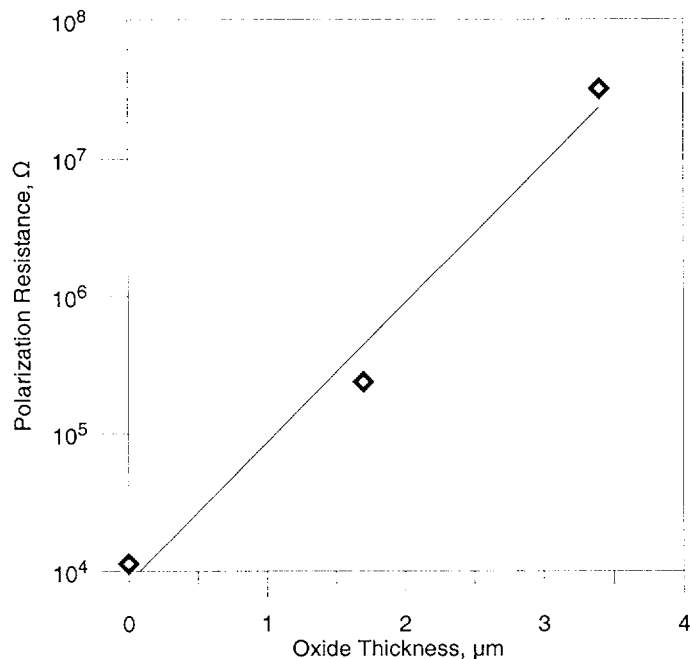


Figure 4: Effect of oxide film thickness on the polarization resistance measured in deaerated 0.1 M Na₂SO₄ solution containing 0.1 M each of FeK₃(CN)₆ and FeK₄(CN)₆. The as-polished condition was assigned a thickness value of 0 μm.

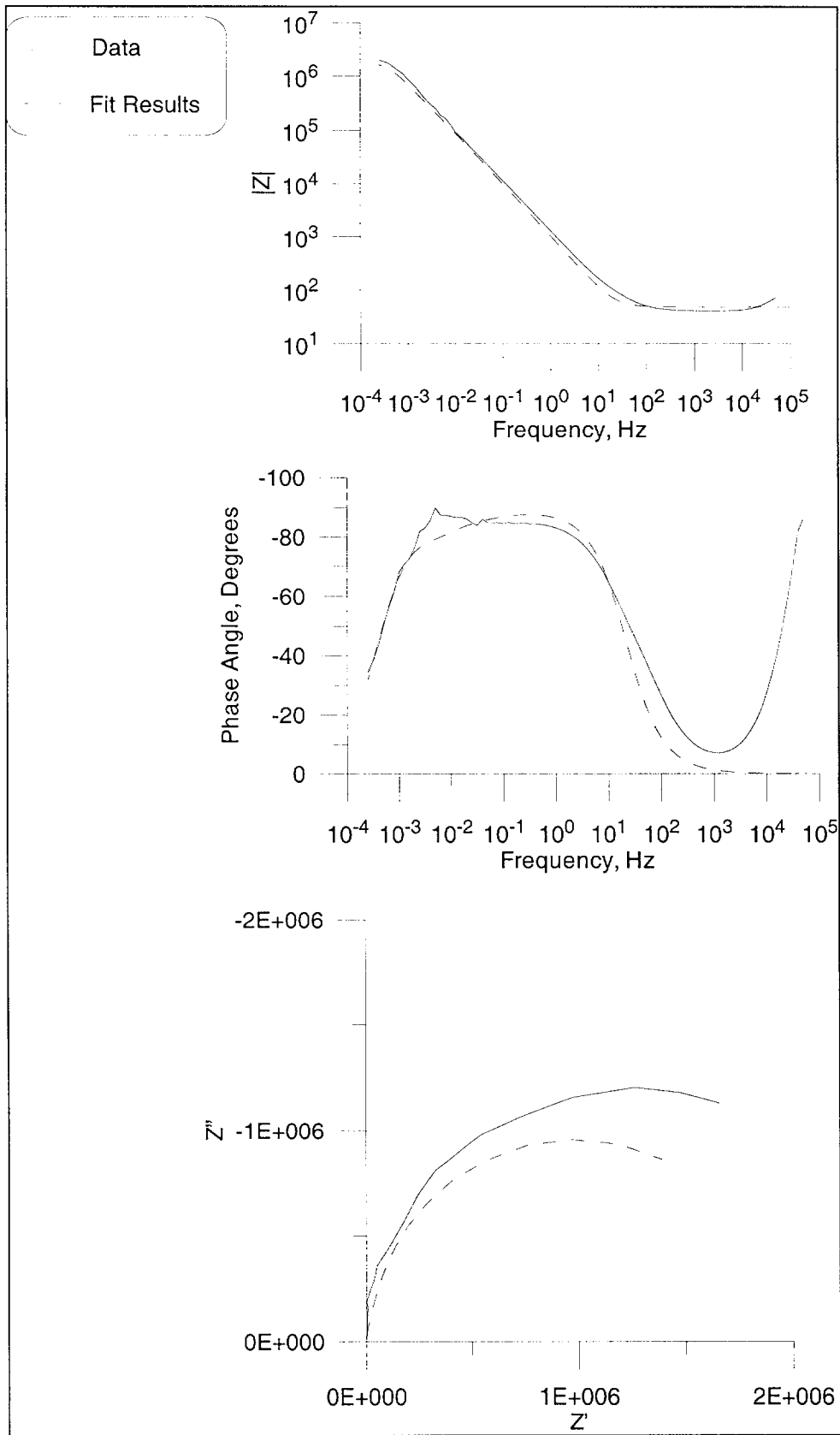


Figure 5: EIS data and fitting results for as-polished Zr-4 in deaerated, 0.1 M NaCl at 95 °C.

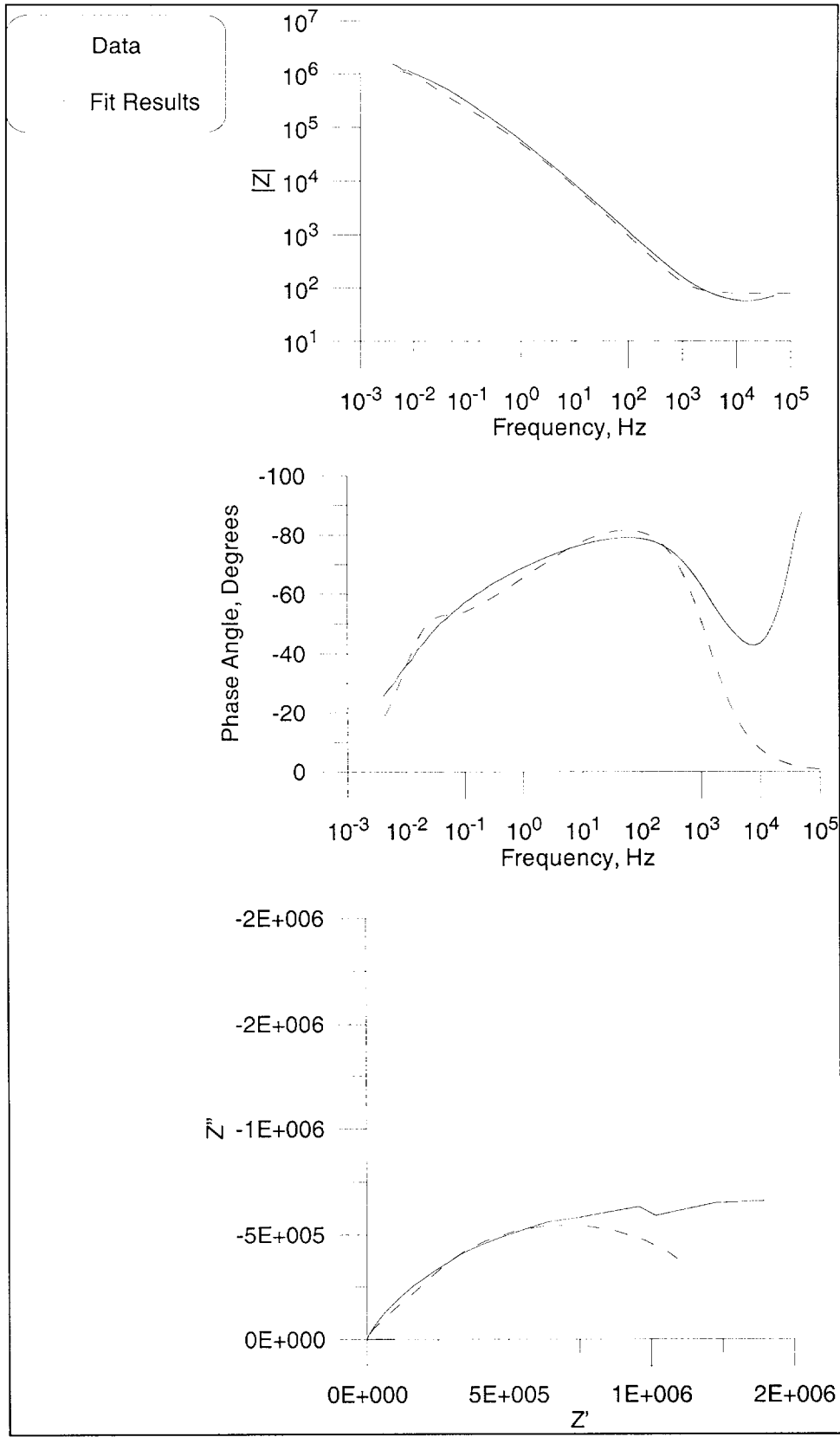


Figure 6: EIS data and fitting results for oxidized Zr-4 with a nominal oxide film thickness of 1.7 μm in deaerated, 0.1 M NaCl at 95 $^\circ\text{C}$.

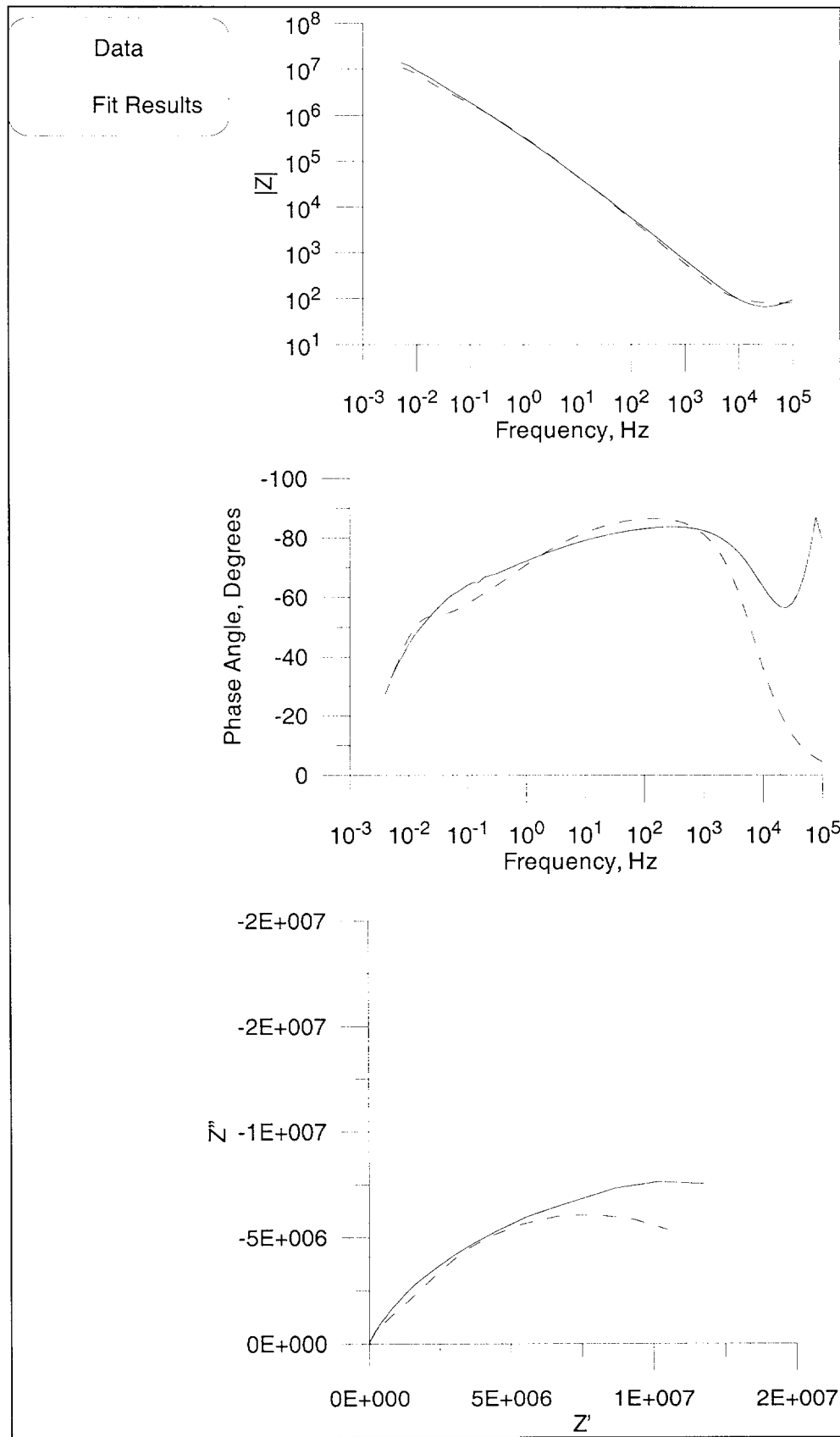


Figure 7: EIS data and fitting results for oxidized Zr-4 with a nominal oxide thickness of $3.4 \mu\text{m}$ in deaerated, 0.1 M NaCl at 95°C .

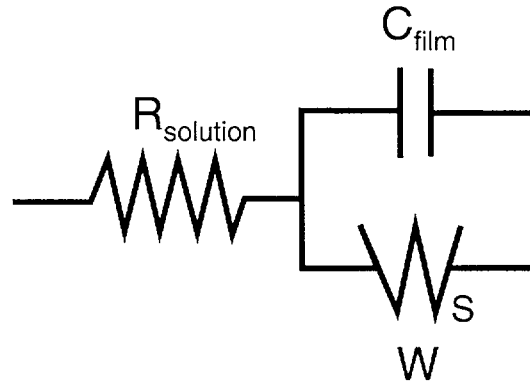


Figure 8: Equivalent circuit used to model EIS results, where R_{solution} is the solution resistance, C_{film} is the oxide film capacitance, and W represents the Warburg impedance.

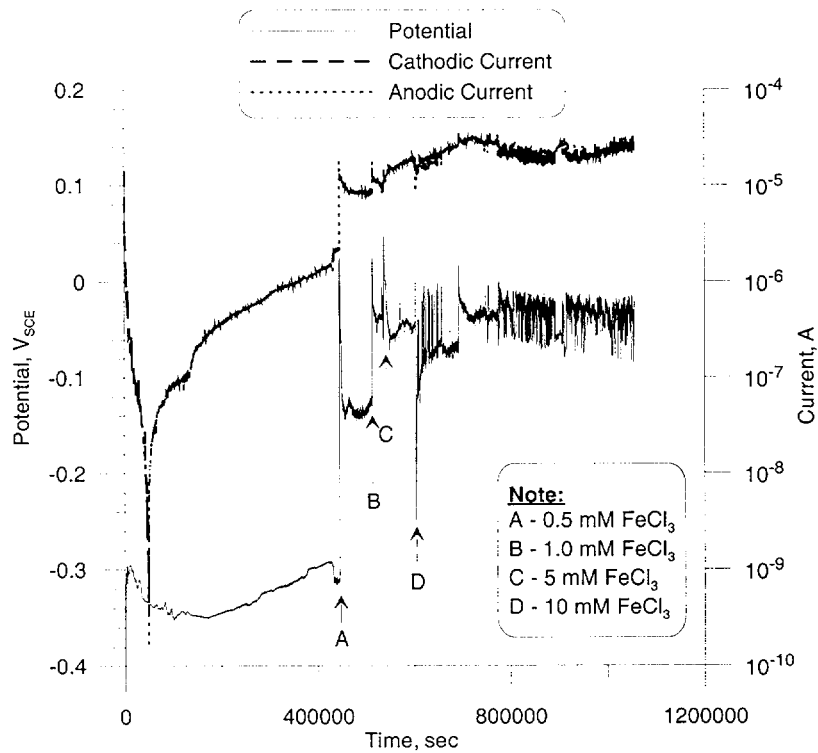


Figure 9: Results from galvanically coupling as-polished Zr-4 with oxidized Zr-4 with an oxide thickness of $3.4 \mu\text{m}$ at an area ratio of 1:10 in air-saturated, 0.1 M NaCl at 25°C with periodic additions of FeCl_3 .